Proc. Natl. Acad. Sci. USA
Vol. 87, pp. 9411–9415, December 1990
Immunology

Expression and chromosomal localization of a lymphocyte K^+ channel gene

(patch clamp/*Xenopus* oocyte/charybdotoxin/polymerase chain reaction)

STEPHAN GRISSMER*, BRENT DETHLEFS†, JOHN J. WASMUTH‡, ALAN L. GOLDIN§, GEORGE A. GUTMAN§, MICHAEL D. CAHALAN*, AND K. GEORGE CHANDY*†¶

Departments of *Physiology and Biophysics, †Medicine, ‡Biological Chemistry, and §Microbiology and Molecular Genetics, University of California, Irvine, CA 92715

Communicated by Erwin Neher, September 4, 1990 (received for review June 18, 1990)

ABSTRACT **We recently isolated a family of three closely related mouse K^+ channel genes (MK1, MK2, and MK3) with coding regions contained in single uninterrupted exons. Here we have used patch-clamp recordings from *Xenopus* oocytes injected with mRNA to show that MK3 encodes a channel with biophysical and pharmacological properties indistinguishable from those of voltage-gated type *n* K^+ channels in T cells. In addition, we used the polymerase chain reaction to demonstrate the presence of MK3 mRNA in T cells. These data suggest that MK3 may encode the T-cell voltage-gated type *n* K^+ channel. We also show that MK3 and MK2 are localized on human chromosomes 13 and 12, respectively.**

Lymphocytes express three distinct types of voltage-gated K^+ channels according to functional subset, the state of activation, and time during development (1–6). These K^+ channels, termed types *n*, *n'*, and *l* (1, 2, 7), are readily distinguished during patch-clamp recording by their voltage dependence of activation, inactivation characteristics, single-channel conductances, and pharmacological specificities. Several lines of evidence suggest that the type *n* K^+ channel in mouse and human T lymphocytes plays an essential role in T-cell proliferation and activation. Expression of type *n* channels is amplified in the most rapidly proliferating thymocyte subsets and in mature cells following mitogen stimulation (3, 4), and K^+ channel blockers inhibit mitogen-induced cell division and secretion of interleukin 2 (6–9). In addition, type *n* channels may underlie K^+ efflux during volume regulation in response to hypotonic osmotic challenge (10, 11).

MK1, MK2, and MK3 comprise a family of Shaker-related K^+ channel genes with intronless coding regions (12). The corresponding homologues from a rat cortex cDNA library have been expressed in oocytes (13). In this study we provide evidence suggesting that the lymphocyte type *n* K^+ channel is encoded by the MK3 gene. The polymerase chain reaction (PCR) amplification procedure was used to show that MK3 is expressed in T cells. Furthermore, expression of the MK3 coding region in *Xenopus* oocytes gives rise to voltage-dependent K^+ currents with gating, conductance, and pharmacological properties that match those of the voltage-gated type *n* K^+ channel. In addition, we used probes prepared from the unique 5′ noncoding region of MK3 (12) to localize MK3 to human chromosome 13.

MATERIALS AND METHODS

Construction and Expression of MK3 in *Xenopus* Oocytes. The MK3 coding region was inserted into the pSP64T cloning vector (14) as follows: MK3 plasmid DNA was cut with *Ban* I, which cuts 9 nucleotides after the ATG initiation codon and 60 nucleotides after the TAA stop codon to generate a 1774-base-pair (bp) fragment containing almost the entire coding region (12). The DNA was filled in with Klenow polymerase and ligated to a synthetic oligodeoxynucleotide (CACGGTCATAGATCTATGACCGTG) that generated the first 9 nucleotides and contained a *Bgl* II recognition site. The fragment was then cut with *Bgl* II (which does not cut within the coding region) and inserted into the single *Bgl* II site in pSP64T. "Minipreps" of plasmid DNA (15) were analyzed for the appropriate orientation by digestion with *Sca* I, and the construction was verified by double-stranded DNA sequencing using the dideoxy chain-termination method (16), with the Sequenase kit (United States Biochemical). For transcription, the plasmid was linearized by digestion with *Eco*RI. RNA was transcribed and injected (70 nl of 0.1 $\mu g/\mu l$) into oocytes as described (17).

Electrophysiology. Experiments were carried out on *Xenopus* oocytes with two-electrode voltage-clamp and patch-clamp techniques (18, 19). All experiments were done at room temperature (22–26°C). For the two-electrode voltage-clamp experiments, cells were bathed in oocyte Ringer solution: 96 mM NaCl/1.8 mM $CaCl_2$/1 mM $MgCl_2$/5 mM Hepes, pH 7.5 adjusted with NaOH. The pipette solution was 3 M KCl. Following verification of K^+ currents with the microelectrode voltage-clamp, patch-clamp experiments were carried out under identical conditions in oocytes and in T cells, using a mammalian Ringer solution: 160 mM NaCl/4.5 mM KCl/2 mM $CaCl_2$/1 mM $MgCl_2$/5 mM Hepes, pH 7.4 adjusted with NaOH; 290–320 mosmol/kg. Internal (pipette) solutions contained 140 mM KF, 2 mM $MgCl_2$, 5 mM Hepes, and 11 mM K_2EGTA. Charybdotoxin (CTX) was a generous gift from Chris Miller (Graduate Department of Biochemistry, Brandeis University, Waltham, MA) and Maria Garcia (Merck Institute, Rahway, NJ).

Data acquisition for patch-clamp experiments was performed as described (2). The holding potential was adjusted in all experiments to −80 mV. Correction for capacitative currents was achieved by analog subtraction. The amplitude of the K^+ current in oocyte patches decreased significantly during outside-out patch recording. The K^+ current amplitude decreased to 53 ± 8% and 34 ± 13% (mean ± SEM; n = 6) after 10 and 20 min, respectively. To correct for run-down, the potency of all blockers was determined as the reduction of the mean K^+ current before and after drug treatment.

Oligonucleotide Primers. Two oligonucleotide primers were prepared (ChemGenes, Needham, MA) from the unique region flanking the loop between the S1 and S2 transmem-

The publication costs of this article were defrayed in part by page charge payment. This article must therefore be hereby marked "*advertisement*" in accordance with 18 U.S.C. §1734 solely to indicate this fact.

Abbreviations: CTX, charybdotoxin; PCR, polymerase chain reaction.

¶To whom reprint requests should be addressed.

brane segments of MK3 (12). The upstream and downstream primers were 5'-GGCATTGCCATTGTGTCAGTGC-3', which spans the S1 transmembrane helix of MK3, and 5'-GAAGCTGGAGGCTCCAGAAGGGG-3', which is the 3' → 5' complement of the unique 3' end of the S1–S2 loop of MK3. A third primer (5'-CGCAGGACGTGTTTGAGGCT-GCC-3') was prepared from the middle of the S1–S2 loop (12).

PCR Amplification of MK3 from EL4 RNA. Total RNA was isolated from the mouse T-cell line EL4 by the guanidinium isothiocyanate method (15) and was used to generate a random-primed cDNA product (20). The 20-μl reaction mixture contained 48 units of avian myeloblastosis virus (AMV) reverse transcriptase (United States Biochemical), 20 units of RNasin (Boehringer Mannheim), 100 pM random hexanucleotide mixture (Boehringer Mannheim), 1 μg of total EL4 RNA, and 1 mM each dinucleoside triphosphate (GeneAmp Kit, Perkin–Elmer/Cetus). In parallel experiments, EL4 RNA was pretreated with boiled RNase A (3 μg; Sigma) and RNase H (3 μg; Pharmacia) for 30 min; the reaction was stopped by the addition of 20 units of RNasin, and cDNA synthesis was initiated. The cDNA product was then amplified for 40 cycles (annealing temperature, 50°C) with *Thermus aquaticus* (*Taq*) DNA polymerase (GeneAmp Kit, Perkin–Elmer/Cetus). The reaction mixture contained 50 pmol of each of the primers and 2 μl of the cDNA template. The amplified product (5–20 μl) was then electrophoresed in a 2.2% agarose gel in Tris acetate/EDTA buffer. Human genomic DNA prepared from the clonal HeLa cell line D98/AH.2 was subjected to PCR analyses under the same conditions. In separate experiments the EL4 cDNA product was amplified for 40 cycles with the primer prepared from the middle of the S1–S2 loop along with the downstream primer, at an annealing temperature of 65°C.

Chromosomal Localization. Since the nearby noncoding regions of MK1, MK2, and MK3 do not share any sequence similarity with each other (12), MK3- and MK2-specific probes were generated from the 5' noncoding regions of these genes, adjacent to the coding regions. A 0.9-kilobase *Hin*dIII–*Pst* I fragment was prepared from the 5' noncoding region of MK2 (12), and a 0.7-kilobase *Pst* I fragment from the 5' noncoding region of MK3 (12). The 5' noncoding regions of these genes share nucleotide sequence similarity with the 5' noncoding regions of RBK2 and RCK3 cDNAs, rat homologues of MK2 and MK3, respectively (13, 21), suggesting that these probes are included in the MK2 and MK3 transcripts (12). These probes were labeled to a specific activity of 10^9 cpm/μg by the random primer method (22) and then used for the chromosomal studies. Chromosomal assignments for MK2 and MK3 loci were determined by Southern blot analysis of a panel of 29 human–Chinese hamster cell hybrids, which were isolated using a variety of selectable markers (23, 24). All hybrids were characterized cytogenetically by trypsin–Giemsa banding (G-banding) and G-11 staining to determine which human chromosomes were retained. The analyses were repeated at the time the cells were harvested for the preparation of DNA. In all cases, 20 metaphase chromosome spreads were examined. The human chromosome content of the hybrids is indicated in Table 2. The presence or absence of human-specific restriction fragments detected by probe MK2 or probe MK3 was correlated with the presence of different human chromosomes in the interspecific cell hybrids.

RESULTS

MK3 Expression in Oocytes. *Xenopus* oocytes express a high density of voltage-activated K^+ channels following injection of MK3 mRNA. With two-electrode voltage clamping, currents in excess of 20 μA at test potentials of +40 mV could be observed (data not shown). Outside-out patches of oocyte membrane were used for measurement of gating kinetics, pharmacological sensitivity, and single-channel properties (Table 1). Reflecting the large currents seen in microelectrode recordings from the whole oocyte, current magnitudes in patches were large, often representing a thousand channels per patch (840 ± 242 K^+ channels per patch; mean ± SEM; n = 11).

Voltage Dependence of MK3. We were struck by the similarity of the oocyte patch currents to whole-cell K^+ currents in human T lymphocytes (6, 9, 25). For comparison of channel properties, identical solutions at mammalian ionic strength were employed in oocyte patches and in lymphocytes. Fig. 1 illustrates records and analysis of K^+ currents from oocytes expressing the MK3 gene product. The outward currents appear to represent a single population of K^+ channels that become activated at potentials positive to about −50 mV. Upon depolarization, the channels open with a sigmoid time course, reach a peak within about 10 ms, and then inactivate with time constants in the range 200–400 ms. From the conductance–voltage relation shown in Fig. 1*B*, the channels are steeply voltage-dependent, with conductances changing e-fold per 4 mV, with a midpoint near −40 mV. These values are also characteristic of K^+ currents recorded in the whole-cell configuration from human and mouse T cells (Table 1). Thus, the voltage dependence for K^+ channel activation of MK3 currents matches that of type n lymphocyte K^+ currents.

Activation and Inactivation Kinetics. Kinetic properties of activation and inactivation are also similar between MK3 currents and n-type currents from lymphocytes. The time

Table 1. Comparison of MK3, RCK3, and RGK5 currents in oocytes with type n currents in T cells

	Gating†				Conductance,‡	Blockers§				
Channel*	V_n, mV	k_n, mV	τ_h, ms	τ_t, ms	pS	TEA, mM	4AP, mM	Qui, μM	Ver, μM	CTX, nM
MK3	−35 ± 4	−6.3 ± 1.4	250 ± 51	55 ± 5	13 ± 1	11	0.4	40	4	0.5, 2.0¶
Type n										
Human	−36	−4.3	178	44	9, 16	8	0.19	14	6	0.5, 1.5¶
Mouse	−36	−7.3	107	49	12–18	10–13	<0.2	4–40	4–40	0.5, 1.5¶
RCK3	−25	−6.6	1.5	—	9.6	50	1.5	—	—	1
RGK5	−14	—	612	—	—	11	0.3	80	30	—

*Values for human T cells from refs. 2, 25, and 26, except for τ_t measured from human peripheral blood T cells (SD = 8, n = 5). Values for mouse T cells from refs. 1 and 2. Values for RCK3 and RGK5 in intact oocytes from refs. 13 and 27, respectively.

†Parameters for channel gating defined in Fig. 1 legend. τ_h reported at 40 mV, τ_t at −60 mV. Values for MK3 are means ± SD (n = 5 except for τ_t, n = 3).

‡Single-channel conductance determined by fitting a line to single-channel events at five potentials. MK3 value is mean ± SD (n = 5).

§Half-blocking doses for tetraethylammonium (TEA), 4-aminopyridine (4AP), quinine (Qui), verapamil (Ver), and CTX, determined by fitting dose–response curves in two to five separate experiments for each blocker.

¶Half-blocking concentration of CTX depended upon the source, as described in ref. 28.

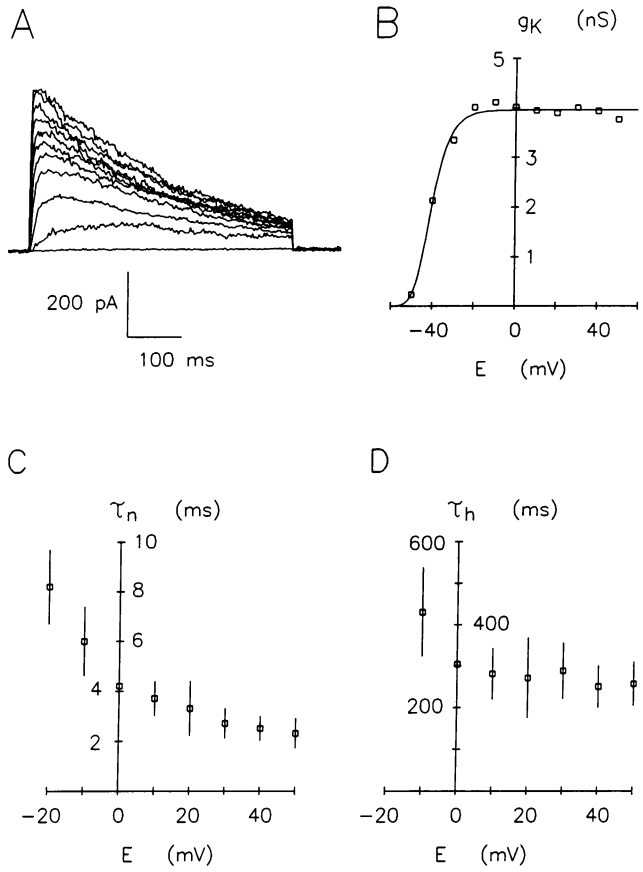

FIG. 1. (*A*) K^+ currents in an outside-out patch from an oocyte injected with MK3 mRNA. The membrane potential was −80 mV, and depolarizing pulses were applied every 45 s. The test potential was changed from −50 to 50 mV in 10-mV increments. (*B*) Peak K^+ conductance–voltage relation for the K^+ currents shown in *A*. The line through the points was fitted with the Boltzmann equation: $g_K(E) = g_{K(max)}/\{1 + \exp[(E_n - E)/k]\}$, with parameter values $g_{K(max)} = 3.9$ nS, $E_n = -40.2$ mV, and $k = -4.0$ mV. (*C* and *D*) Activation (*C*) and inactivation (*D*) time constants, τ_n and τ_h, were obtained by fitting curves through the current data points of similar traces as shown in *A* according to a Hodgkin–Huxley type n^4h model: $I_{total} = I_{K(max)}[1 - \exp(-t/\tau_n)]^4 \exp(-t/\tau_h)$. The points in *C* and *D* represent averages (±SD) of τ_n and τ_h obtained from five different patches.

course of K^+ currents in five oocyte patches was analyzed by use of a modified Hodgkin–Huxley kinetic model with activation (n^4) and inactivation (h), as previously described for lymphocytes (25); no particular mechanism for gating is implied. Fig. 1 *C* and *D* illustrate K^+ channel kinetics of opening and inactivation for the MK3 gene expressed in oocytes. The rates for channel activation and inactivation are similar to those in human T lymphocytes (Table 1). Channel inactivation, in particular, provides a convenient property to distinguish between diverse types of K^+ channels. Inactivation of type *n* lymphocyte channels progresses with a rate in between classically defined A currents, which inactivate in <100 ms, and delayed rectifiers, which inactivate with time constants >1 sec (reviewed in refs. 28 and 29). Moreover, inactivation of type *n* channels accumulates during repetitive depolarizing pulses delivered at 1 Hz, because recovery during the interpulse interval is incomplete. Both the time course and use dependence of inactivation exhibited by MK3 K^+ currents expressed in oocytes are similar to those in the lymphocyte (Figs. 1*D* and 2*A*; Table 1). Finally, channel closing upon repolarization is similar between type *n* K^+ currents and the MK3 gene product expressed in oocytes (Fig. 2*B* and Table 1).

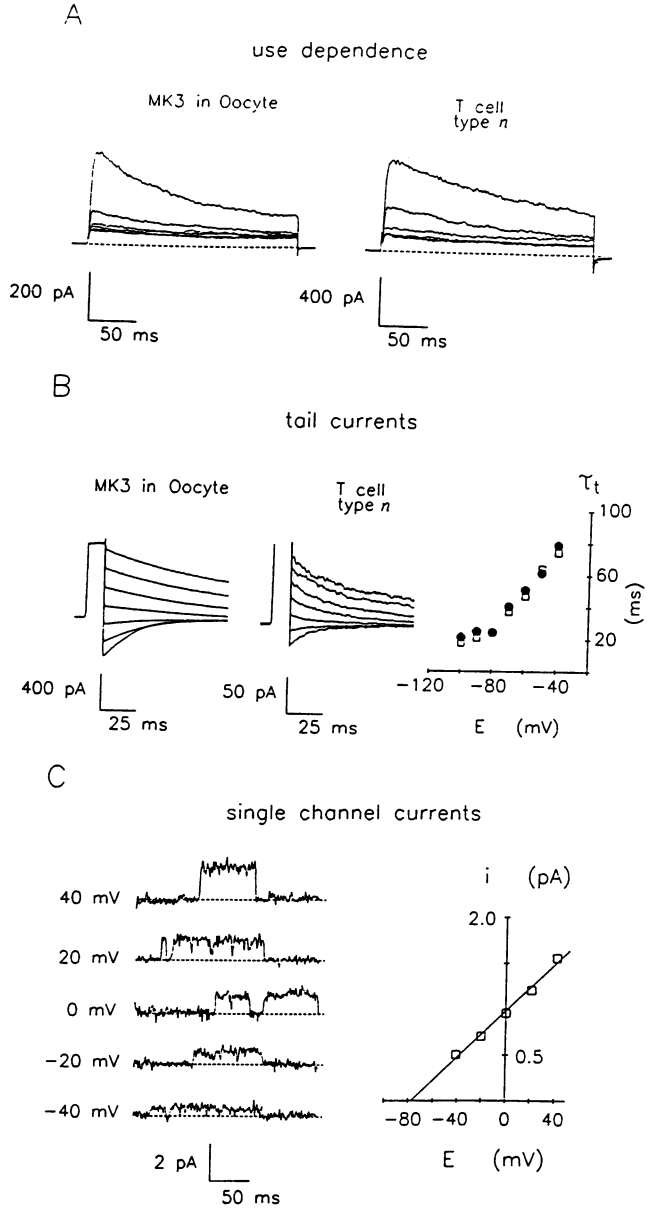

FIG. 2. Comparison of the biophysical properties of MK3 and the type *n* K^+ channel. (*A*) Cumulative (use-dependent) inactivation of MK3 K^+ currents in an outside-out patch from an oocyte injected with MK3 mRNA (*Left*) and of K^+ currents obtained from a human peripheral blood lymphocyte (*Right*). Currents were elicited by a train of six depolarizing voltage steps to 40 mV once every second from a holding potential of −80 mV. The test pulse duration was 200 ms. The K^+ current amplitude decreases substantially during this train of pulses from largest (first) to smallest (last). (*B*) Kinetics of deactivation of MK3 K^+ currents in an outside-out patch from an oocyte injected with MK3 mRNA (*Left*) and of K^+ currents obtained from a human peripheral blood lymphocyte (*Center*). Tail currents were elicited by voltage steps from −100 to −40 mV after a 15-ms depolarizing prepulse to 40 mV. Tail current-decay time constants, τ_t, were fitted with single exponentials and plotted vs. the applied membrane potential, E, during the decay (*Right*). The filled circles represent τ_t for MK3; the open squares represent τ_t for the T cell. (*C*) Single-channel currents of MK3 K^+ currents in an outside-out patch from an oocyte injected with MK3 mRNA. (*Left*) The membrane potential was held at the potentials indicated to the left of the current traces. After most of the channels in the patch inactivated, single-channel currents of different amplitudes at the different holding potentials could be monitored. (*Right*) Current amplitude produced by the opening of single channels is plotted vs. holding potential. The slope of the line gives an estimate of 13 pS for the single-channel conductance; the line intercepts the voltage axis at −76 mV, close to the equilibrium potential for K^+ ions.

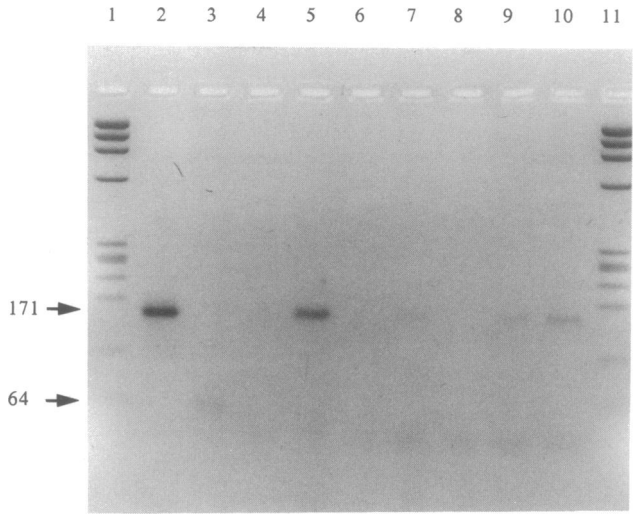

FIG. 3. Amplification of 171- and 64-bp fragments from EL4 RNA. Lanes 1 and 11: molecular size markers, ϕX174 (New England Biolabs); the sizes of the standards are 1353, 1078, 872, 603, 310, 281, 271, 234, 194, 118, and 72 bp. Lanes 2 and 3: the 171- and 64-bp fragments amplified from EL4 RNA; 20 μl of PCR product was loaded in these lanes. Lanes 4–10: liver, spleen, atrium, kidney, ventricle, cortex, and fibroblasts, respectively.

Single-Channel Conductance. Measurements of single-channel conductance strengthen the identification of MK3 as the gene that encodes the lymphocyte type *n* K^+ channel. In an oocyte patch containing many K^+ channels, it is possible to measure single-channel currents by holding the membrane potential at various depolarized levels. As inactivation proceeds, single-channel currents eventually can be seen (Fig. 2*C*). These currents correspond to a single-channel conductance of about 13 pS, similar to values of 9 and 16 pS reported in human T cells (25), and 13 and 18 pS in mouse T cells (1, 2).

MK3 and Type *n* K^+ Channels Share Similar Pharmacological Properties. Block by pharmacological agents is another means of classifying K^+ channels. Type *n* K^+ channels from human and mouse lymphocytes are sensitive to block by a wide spectrum of agents (6, 8, 9, 25, 26) including (in increasing order of potency) tetraethylammonium, 4-aminopyridine, quinine, verapamil, and CTX. Oocyte K^+ currents following injection of MK3 mRNA exhibit the same pharmacological specificities (Table 1).

MK3 Is Expressed in EL4 T Cells. EL4 T cells exhibit voltage-gated type *n* K^+ channels (≈200 per cell) together with inward rectifier K^+ channels (30). Total RNA from these cells was reverse transcribed and analyzed by PCR. We chose to make primers from the loop linking the S1 and S2 transmembrane helices of MK3, since this region has a unique sequence that distinguishes it from even the closely related MK1 and MK2 genes (12). MK3 specificity of these primers was confirmed by comparing their sequences with those available at GeneBank. Two fragments that were predicted from the sequence of the MK3 S1–S2 loop, 171 bp and 64 bp in size, were amplified from EL4 RNA (Fig. 3). The 171-bp fragment was also expressed in spleen, kidney, cortex and fibroblasts, but not in liver, atria, or ventricles (Fig. 3). To test whether this fragment was derived from EL4 RNA or from possible contaminating genomic DNA, we pretreated EL4 RNA with DNase-free RNase A and H (to degrade RNA without affecting DNA) and then performed PCR. We were unable to amplify the 171-bp fragment from RNase-treated EL4 RNA in two separate experiments (data not shown), indicating that the fragment was derived from the RNA, rather than from any possible genomic DNA contaminant. As additional controls, cDNA from liver, atria, and ventricles and genomic DNA derived from HeLa cells were subjected to PCR analyses at the same time and under identical conditions; we were unable to amplify the 171-bp fragment (data not shown). Furthermore, since EL4 cells are clonal, the RNA prepared from these cells was unlikely to be derived from a contaminating cell type. Collectively, these data indicate that MK3 is expressed in EL4 T cells and in spleen, kidney, brain, and fibroblasts.

Chromosomal Localization. Based upon Southern blot analysis of a panel of 29 human–Chinese hamster cell hybrids, MK2 was assigned to human chromosome 12 and MK3 was assigned to human chromosome 13 (Table 2). MK2 was 100% concordant with chromosome 12 and MK3 was 100% concordant with chromosome 13.

DISCUSSION

We have used two approaches to investigate the molecular identity of the type *n* K^+ channel in T lymphocytes. The first was to compare its biophysical properties with currents in an oocyte following injection of MK3 mRNA, using identical solutions in patch-clamp experiments (summarized in Table 1). We examined the voltage dependence of opening, inactivation, and closing; conductance properties; and pharmacological sensitivity of the channel encoded by the MK3 gene, and found that these properties of the MK3 gene closely resemble those of type *n* K^+ channels in both mice and humans (Table 1). Among previously described voltage-gated K^+ channels, the combination of voltage dependence, inactivation rate, cumulative inactivation, and CTX sensitivity is unique for type *n* channels and serves to distinguish the MK3 gene product from type *n'* or *l* channels in lymphocytes. We used PCR as a second approach to demonstrate that MK3 is transcribed and expressed in T cells. Using oligonucleotide primers derived from the unique S1–S2 interdomain region of MK3, we amplified 171-bp and 64-bp fragments from T-cell RNA that was predicted from the MK3 sequence (12). Based on these data, we conclude that MK3 encodes type *n* K^+ channels from lymphocytes.

RCK3, the rat cDNA homologue of MK3, hybridizes with a 9.5-kilobase mRNA in the brain (13, 31). In addition, RGK5, the rat genomic homologue of MK3, hybridizes with a similarly sized message in mouse thymus (27). Using PCR, we have demonstrated MK3 in a T-cell line, in fibroblasts, and in cortex, spleen, and kidney, but not in liver or heart. Thus, the same K^+ channel subunits appear in several different tissues. Not surprisingly, considering their structural similarity, MK3 currents are remarkably similar to those of RCK3 and RGK5 (13, 27); reported variations in kinetic and pharmacological properties may reflect the differences in

Table 2. Localization of MK2 and MK3 on human chromosomes

	No. of discordant clones																							
Probe	1	2	3	4	5	6	7	8	9	10	11	12	13	14	15	16	17	18	19	20	21	22	X	Y
MK2	8	6	10	4	22	11	2	11	6	5	8	0*	9	12	7	5	7	10	11	7	10	5	6	6
MK3	4	4	9	7	22	9	7	10	6	7	8	9	0*	7	6	8	6	10	10	6	11	8	7	6

*DNA from every clone that contained chromosome 12 hybridized to the MK2 probe; therefore the discordancy of chromosome 12 for MK2 is zero. Similarly, the discordancy of chromosome 13 for MK3 is zero.

experimental conditions when intact oocytes are compared with outside-out patches. K^+ channel subunits related to the Shaker family are able to assemble in *Xenopus* oocytes as homo- or heteromultimers (32, 33). Our results indicate that the biophysical properties of MK3 homomultimers in oocyte patches are indistinguishable from those of type *n* channels in lymphocytes, except that the oocyte patch currents run down more rapidly. It is possible that additional channel subunits in lymphocytes may help to stabilize functional channels.

MK1, MK2, and MK3 share about 70% coding-region sequence identity, although their nearby noncoding regions do not share any discernible sequence similarity (12). All three genes have coding regions that are contained in single uninterrupted exons, and comprise a gene family that probably arose by gene duplication from a common ancestor (12). Members of closely related gene families are often located together on a chromosome. To examine whether MK1–3 are organized in this fashion, we used MK2- and MK3-specific noncoding-region probes (12) to ascertain the chromosomal location of these two genes. Surprisingly, MK2 and MK3 are on separate chromosomes, MK2 on human chromosome 12 and MK3 on human chromosome 13. The three isoforms of the α subunit of the γ-aminobutyrate type A receptor are similarly located on three different chromosomes (34). Retroviruses and retrotransposons have been hypothesized to insert processed genes into the eukaryotic genome, giving rise to diverse chromosomal locations for closely related genes (35). However, MK1–3 have introns within the 5′ noncoding regions (12) and therefore are not processed. Thus, retroviral or retrotransposon insertion events are unlikely to account for the different chromosomal locations of MK2 and MK3.

Type *n* K^+ channel expression varies during mouse T-cell development in parallel with the rate of cell division (1, 4). Immature proliferating thymocytes display ≈200 type *n* K^+ channels per cell (1), the number decreasing to about 10–20 per cell during differentiation into mature, quiescent T cells (1, 5). Activation of mature T cells results in a 20-fold increase in K^+ channel number, the increase being exclusively of type *n* (3). The molecular mechanisms responsible for these changes in type *n* K^+ channel expression are not understood. Future characterization of the MK3 gene and its regulatory elements during T-cell development and activation may clarify these issues.

We thank Drs. Chris Miller and Maria Garcia for providing CTX, Dr. Dennis Heck for advice and help with PCR, Mr. Randy Wymore for preparing EL4 RNA, Mr. Sanjiv Ghanshani for preparing noncoding probes for MK2 and MK3, and Ms. Linda Hall for help with chromosomal localization. We are grateful to Dr. Synnöve Beckh and Ruth Davis for helpful comments on the manuscript. This work was supported by National Institutes of Health Grants AI24783 (K.G.C.), AI21366 (G.A.G.), NS26729 (A.L.G.), NS14609 (M.D.C.), and GM42365 (J.J.W.); a grant from Pfizer (Groton, CT) (K.G.C.); the Office of Naval Research (M.D.C.); a Markey Scholar Award (A.L.G.); a March of Dimes Basil O'Connor Award (A.L.G.); an award from the Alexander von Humboldt Foundation (M.D.C.); and Juvenile Diabetes Foundation Grant 188209 (G.A.G.).

1. Lewis, R. S. & Cahalan, M. D. (1988) *Science* **239,** 771–775.
2. DeCoursey, T. E., Chandy, K. G., Gupta, S. & Cahalan, M. D. (1987) *J. Gen. Physiol.* **89,** 379–404.
3. DeCoursey, T. E., Chandy, K. G., Gupta, S. & Cahalan, M. D. (1987) *J. Gen. Physiol.* **89,** 405–420.
4. McKinnon, D. & Ceredig, R. (1986) *J. Exp. Med.* **164,** 1846–1861.
5. Grissmer, S., Cahalan, M. D. & Chandy, K. G. (1988) *J. Immunol.* **141,** 1137–1142.
6. DeCoursey, T. E., Chandy, K. G., Gupta, S. & Cahalan, M. D. (1984) *Nature (London)* **307,** 465–468.
7. Chandy, K. G., DeCoursey, T. E., Fischbach, M., Talal, N., Cahalan, M. D. & Gupta, S. (1986) *Science* **233,** 1197–1200.
8. Chandy, K. G., DeCoursey, T. E., Cahalan, M. D., McLaughlin, C. & Gupta, S. (1984) *J. Exp. Med.* **160,** 369–385.
9. DeCoursey, T. E., Chandy, K. G., Gupta, S. & Cahalan, M. D. (1985) *J. Neuroimmunol.* **10,** 71–95.
10. Cahalan, M. D. & Lewis, R. S. (1988) in *Cell Physiology of Blood,* eds. Gunn, R. & Parker, J. (Rockefeller Univ. Press, New York), pp. 208–301.
11. Grinstein, S. & Smith, J. D. (1990) *J. Gen. Physiol.* **95,** 97–120.
12. Chandy, K. G., Williams, C. B., Spencer, R. H., Aguilar, B. A., Ghanshani, S., Tempel, B. L. & Gutman, G. A. (1990) *Science* **247,** 973–975.
13. Stühmer, W., Ruppersberg, J. P., Schröter, K. H., Sakmann, B., Stocker, M., Giese, K. P., Perschke, A., Baumann, A. & Pongs, O. (1989) *EMBO J.* **8,** 3235–3244.
14. Krieg, P. A. & Melton, D. A. (1984) *Nucleic Acids Res.* **12,** 7057–7070.
15. Maniatis, T., Fritsch, E. F. & Sambrook, J. (1982) *Molecular Cloning: A Laboratory Manual* (Cold Spring Harbor Lab., Cold Spring Harbor, NY).
16. Sanger, F., Nicklen, S. & Coulson, A. R. (1977) *Proc. Natl. Acad. Sci. USA* **74,** 5463–5467.
17. Auld, V. J., Goldin, A. L., Krafte, D. S., Marshall, J., Dunn, J. M., Catterall, W. A., Lester, H. A., Davidson, N. & Dunn, R. J. (1988) *Neuron* **1,** 449–461.
18. Hamill, O. P., Marty, A., Neher, E., Sakmann, B. & Sigworth, F. J. (1981) *Pflügers Arch.* **391,** 85–100.
19. Methfessel, C., Witzemann, V., Takahashi, T., Mishina, M., Numa, S. & Sakmann, B. (1986) *Pflügers Arch.* **407,** 577–588.
20. Krug, M. S. & Berger, S. L. (1987) *Methods Enzymol.* **152,** 316–325.
21. McKinnon, D. (1989) *J. Biol. Chem.* **264,** 8230–8236.
22. Feinberg, A. P. & Vogelstein, B. (1983) *Anal. Biochem.* **132,** 6–13.
23. Cirullo, R. E., Arrendo-Vega, F. X., Smith, M. & Wasmuth, J. J. (1983) *Somatic Cell Genet.* **9,** 215–233.
24. Overhauser, J., McMahon, J. & Wasmuth, J. J. (1987) *Nucleic Acids Res.* **15,** 4617–4627.
25. Cahalan, M. D., Chandy, K. G., DeCoursey, T. E. & Gupta, S. (1985) *J. Physiol.* **358,** 197–237.
26. Sands, S. B., Lewis, R. S. & Cahalan, M. D. (1989) *J. Gen. Physiol.* **93,** 1061–1074.
27. Douglass, J., Osborne, P. B., Cai, Y.-C., Wilkerson, M., Christie, M. J. & Adelman, J. P. (1990) *J. Immunol.* **144,** 4841–4850.
28. Hille, B. (1984) *Ionic Channels of Excitable Membranes* (Sinauer, Sunderland, MA).
29. Rudy, B. (1988) *Neuroscience* **25,** 729–749.
30. Cahalan, M. D., Chandy, K. G., DeCoursey, T. E., Gupta, S., Lewis, R. S. & Sutro, J. (1987) *Adv. Exp. Med. Biol.* **213,** 85–102.
31. Beckh, S. & Pongs, O. (1990) *EMBO J.* **9,** 777–782.
32. Isacoff, E. Y., Jan, Y. N. & Jan, L. Y. (1990) *Nature (London)* **345,** 530–534.
33. Ruppersberg, J. P., Schröter, K. H., Sakmann, B., Stocker, M., Sewing, S. & Pongs, O. (1990) *Nature (London)* **345,** 535–537.
34. Buckle, V. J., Fujita, N., Ryder-Cook, A. S., Derry, J. M. J., Barnard, P. J., Lebo, R. V., Schofield, P. R., Seeburg, P. H., Bateson, A. N., Darlison, M. G. & Barnard, E. A. (1989) *Neuron* **3,** 647–654.
35. Weiner, A. M., Deininger, P. L. & Efstratiadis, A. (1986) *Annu. Rev. Biochem.* **55,** 631–661.